Cloud–rain predator–prey interactions: Analyzing some propertiesof the Koren–Feingold model and introduction of a new species-competition bulk system with a Hopf bifurcation

Olivier Pujol, Andrew Jensen

Version of Record: https://www.sciencedirect.com/science/article/pii/S0167278918301520
Manuscript_a56398ec5e958c1894ae8ab64368e960

Cloud-rain predator-prey interactions: analyzing some properties of the Koren-Feingold model and introduction of a new species-competition bulk system with a Hopf bifurcation

Olivier Pujol[a,*], Andrew Jensen[b]

[a] *Université de Lille, Département de Physique, Laboratoire d'Optique Atmosphérique, 59655, Villeneuve d'Ascq, France*
[b] *Mathematical Sciences, Northland College, Ashland, 54806, WI, USA*

Abstract

This paper deals with some properties of predator-prey cloud-rain models. Focus is put on scaling and on some mathematical features such as stability and limit cycles. Precisely, the Koren-Feingold delay differential equation model is first investigated and it is shown that it has no limit cycles. Then, by considering another point of view (*i.e.* species competition dynamics) for parametrizing cloud-rain processes, a system of ordinary differential equations to model these processes is formulated. Some examples are given to illustrate that this model reproduces in a realistic way the essential macroscopic behavior of a cloud-rain system. The model has a Hopf bifurcation at which certain properties of cloud-rain interactions in the model are represented. This is an important point to prepare for further examination of cloud synchronization in a cloud field by Kuramoto model, for instance.

Keywords: Cloud-rain interactions, Species competition dynamics, Predator-prey model, Cloud physics

∗. Corresponding author
Email addresses: olivier.pujol@univ-lille.fr (Olivier Pujol), ajensen@northland.edu (Andrew Jensen)

1. Introduction

Clouds are complex nonlinear dynamic systems with many degrees of freedom and interactions across a vast range of spatio-temporal scales. Despite this complexity, certain non-trivial aspects of their macrobehavior are predictable without a consideration of the full complexity of the dynamic system (Feingold et al., 2010; Koren and Feingold, 2011; Feingold and Koren, 2013; Koren et al., 2017; Mülmenstädt and Feingold, 2018). This implies that models that capture the essential physics have the potential to contribute to our understanding of clouds and their interactions. Such models are thus always welcome, especially in conjunction with more detailed models. This is of importance in the context of the climate system (*e.g.* Held, 2005) since, as is well known, clouds play a major role in the climate system (IPCC, 2013).

An example of macrobehavior that can be tackled by nonlinear dynamics is the interaction between cloud droplets and rain. Recently, Koren and Feingold (2011) (hereafter KF11) analyzed cloud-rain coupling by means of the following non-linear system of delay differential equations (DDEs):

$$\begin{cases} \dfrac{\mathrm{d}H}{\mathrm{d}t} &= \dfrac{H_0 - H}{\tau_1} - \dfrac{\alpha H^2(t-T)}{c_1 N_d(t-T)} \\ \dfrac{\mathrm{d}N_d}{\mathrm{d}t} &= \dfrac{N_0 - N_d}{\tau_2} - \alpha c_2 H^3(t-T) \end{cases} \tag{1}$$

with $c_1 = 2 \times 10^{-6}\,\mathrm{mm\,m^{-2}}$, $c_2 = 0.3\,\mathrm{m^{-1}}$, and $\alpha = 2\,\mathrm{mm\,m^{-6}\,d^{-1}}$ (see also Table 1 in appendix). Here, H is cloud depth (in m) and N_d is cloud droplet concentration (in $\mathrm{cm^{-3}}$). These are the two macroscopic degrees of freedom. In addition, t is time and T is an arbitrary constant delay (both in minutes). The constants τ_1 and τ_2 are timescales of the order of ten minutes. H_0 is a height that represents the full environmental potential for cloud development (*i.e.* the maximum cloud depth possible) and N_0 is the background concentration of aerosol (*i.e.* the maximum concentration of cloud droplets that can be reached). According to KF11, this system exhibits predator-prey like behavior. In particular, two examples of cloud behavior are provided which represent (*i*) an oscillator limit cycle and (*ii*) a damped oscillator.

In the first part of this paper, we explore some physical and mathematical properties of Eq.1 that we consider important from the perspective of nonlinear dynamics that have thus far not been addressed. More precisely, our analysis, which is presented in Section 2, concentrates on scale analysis,

form of the equations, stability analysis, and the question of the existence of limit cycles by means of the Busenberg theorem applied to DDEs.

In the second part of this paper, we introduce a bulk model which follows the initial idea of modeling the macrobehavior of a cloud-rain system and has properties in common with species competition dynamics. In contrast to the KF11 model, it is a system of ODEs rather than DDEs. However, the model presented here reproduces the behavior of the KF11 model, and is derived from a physically-based parametrization. This model differs from the KF11 model not only in its structure, but in the variety of its dynamics which we examine through the lense of nonlinear dynamics, *e.g.* linear stability analysis and bifurcation theory. This exploration yields regions of parameter space in which clouds grow at the expense of rain and *vice versa*.

It must be emphasized that this model does not consider the full complexity of cloud-precipitation interactions; rather, we examine certain predictable elements of the macrobehavior of the full complex dynamical system. In particular, the model we propose incorporates population dynamics in a natural way, which includes exchanges with the surrounding environment. Our model is presented in Section 3 and examples are given in order to show that it is physically realistic and able to reproduce the macroscopic behavior of a cloud-rain system. Section 4 provides a discussion and conclusions.

2. Analysis of some physical and mathematical properties of the KF11 model

2.1. Scale or order-of-magnitude analysis

The system (1) can be solved numerically by means of the pydelay package of Python (`http://pydelay.sourceforge.net/`) or MATLAB's dde23 algorithm. The PyDDE solver can also be useful. These methods are based on the Bogacki-Shampine method which is a 3(2) Runge-Kutta scheme adapted to DDEs. However, before diving into numerical computations, we analyze the magnitudes of the different terms in the system of equations.

In order to have a consistent set of equations in terms of units, we replace α and c_2 in Eq. (1) by $\alpha' = 10^{-3}\,\alpha/(60\times 24)$ and $c_2' = 10^{-6}\,c_2$ (see appendix). Typically, for cloud height, $H_0 \sim 500\,\mathrm{m}$ and so, by definition of H_0, $0 < H < H_0$. For cloud droplet concentration, $N_0 \sim 400\,\mathrm{cm}^{-3}$ and so, by definition of N_0, $N_d < N_0$. A reasonable minimum for N_d ($N_{d,min}$) is about $50\,\mathrm{cm}^{-3}$. Hence, considering the values of the constants involved in Eq. (1), *i.e.* $\tau_1 =$

$\tau_2 \sim 60\,\mathrm{min}$, we find:

$$\frac{H_0 - H}{\tau_1} < \frac{H_0}{\tau_1} \approx 8\,\mathrm{m\,min^{-1}} \qquad \frac{\alpha' H^2}{c_1 N_d} < \frac{\alpha' H_0^2}{c_1 N_{d,min}} \approx 3\,500\,\mathrm{m\,min^{-1}}$$

and

$$\frac{N_0 - N_d}{\tau_2} < \frac{N_0}{\tau_2} \approx 7\,\mathrm{cm^{-3}\,min^{-1}} \qquad \alpha' c_2' H^3 < \alpha' c_2' H_0^3 \approx 0.5\,\mathrm{cm^{-3}\,min^{-1}}$$

It follows that, since H and N_d are physically expected to maintain orders or magnitude as mentioned above during the evolution of the cloud rain system, that $\alpha' H^2/(c_1 N_d)$ and $(N_0 - N_d)/\tau_2$ are the dominant terms in Eq. (1). This is particularly clear for the equation governing the evolution of H. Concerning the equation for $\mathrm{d}N_d/\mathrm{d}t$, having a ratio close to 1 implies that c_2 be 10^4 or 10^5 higher than the value given in Table 1. Consequently, the evolution of N_d is either an increasing or a decreasing exponential function according to the sign (positive or negative, respectively) of $N_0 - N_d$. The examples chosen by KF11 have positive signs. Precisely, $N_d(t) - N_0 = [N_d(0) - N_0]\,\exp(-t/\tau_2)$, where $N_d(0) = N_d(t = 0)$. It ensues that N_d evolves exponentially towards N_0. With respect to $\mathrm{d}H/\mathrm{d}t$, the dominant term is always negative and, unless N_d becomes very small, it will remain the dominant term in the evolution of H. Hence, H is a decreasing function which must stop at $H = 0$ by definition. This scale analysis, based only on the physical realistic orders of magnitude of H and N_d is independent of any constant delay in the equation. Some numerical computations with the numerical scheme mentioned above have confirmed the evolution described above (Fig. 1). Nonetheless, we have obtained some oscillatory behavior in rare cases by varying arbitrarily some constants in Eq. (1) as the constant c_1 around $10^{-3}\,\mathrm{mm\,m^{-1}}$ and the constant c_2 around $10^4\,\mathrm{m^{-1}}$ or $10^5\,\mathrm{m^{-1}}$. We have observed that these oscillations are, in addition, extremely sensitive to the value of c_2 chosen since they disappear if c_2 is changed even slightly (we recover the evolution described above).

2.2. Form of the system of equations

It is worth noting that the system (1) of two equations is not formally similar to a predator-prey system, *stricto sensu*. Indeed, in its basic form, the Lokta-Volterra system is the following (x and y are the two degrees of

freedom):

$$\begin{cases} \dfrac{\mathrm{d}x}{\mathrm{d}t} &= \quad ax - bxy \\ \dfrac{\mathrm{d}y}{\mathrm{d}t} &= -cy + dxy \end{cases} \tag{2}$$

with $\{a, b, c, d\}$ a set of four positive constants. The signature $(+, - \mid -, +)$, or sometimes $(+, - \mid +, -)$, is also present in more elaborate versions of Lokta-Volterra models (*e.g.* Lipowski and Lipowska, 2000) since it is a characteristic of species-competition models, with or without predation. However, the system 1 has the form: $\mathrm{d}H/\mathrm{d}t = -AH - BH^2/N_d$ and $\mathrm{d}N_d/\mathrm{d}t = -CN_d - DH^3$ with $\{A, B, C, D\}$ a set of four positive constants. So, system (1) does not have the general form of a Lokta-Volterra system since the signature is fully negative, $(-, - \mid -, -)$. It follows that $\dot{H}$ and $\dot{N}_d$ are negative if (H, N_d) always satisfy the two inequalities:

$$\frac{H}{\tau_1} + \frac{\alpha' H^2}{c_1 N_d} > \frac{H_0}{\tau_1} \sim 10\,\mathrm{m\,min^{-1}}$$

and

$$\frac{N_d}{\tau_2} + \alpha' c_2' H^3 > \frac{N_0}{\tau_2} \sim 1 - 10\,\mathrm{cm^{-3}\,min^{-1}}$$

So, with regard to the typical orders of magnitude of the two degrees of freedom ($H \sim 400\,\mathrm{m}$, $N_d \sim 100\,\mathrm{cm^{-3}}$), care is needed in the choice of the constants (*i.e.* in the model parametrization) in order to avoid always decreasing functions $H(t)$ and $N_d(t)$.

2.3. Stability analysis

To determine further some of the properties of the system (1), we briefly discuss the stability of the model (with no delay) near its equilibrium points. These are independent of any delays, so that a system of DDEs has the same equilibrium points as the corresponding system (zero delay) of ODEs. However, investigating the stability for DDEs is a more complex task (*e.g.* Engelborghs et al., 2000, and references therein) which is beyond the scope of this paper (some elements can be found in Koren et al. (2017, Section IV)). Nonetheless, it is still instructive to analyze stability in the simplest case of no delay. A quick calculation yields that the KF11 system has an equilibrium point given by

$$N_d^e = N_0 - \alpha' c_2' \tau_2 (H^e)^3$$

and

$$H^e = \frac{c_1 N_d^e}{2\alpha' \tau_1} \left[-1 + \left(1 + \frac{4\alpha' \tau_1 H_0}{c_1 N_d^e} \right)^{1/2} \right] \tag{3}$$

Physically, because N_d^e (and H^e) must be positive, the value of $\alpha' c_2'$ is constrained: $\alpha' c_2' < N_0/[\tau_2 (H^e)^3]$. The behavior of Eq. (1) near this equilibrium point can be obtained by evaluating the Jacobian matrix J at (H^e, N_d^e) and finding its eigenvalues. These are given by the well-known formula:

$$\lambda_\pm = \frac{1}{2} \left[T_J \pm \left(T_J^2 - 4\Delta_J \right)^{1/2} \right]$$

where T_J and Δ_J are respectively the trace and the determinant of $[J]$. A straightforward calculation yields:

$$T_J = -\left(\frac{1}{\tau_1} + \frac{1}{\tau_2} + \frac{2\alpha' H^e}{c_1 N_d^e} \right)$$

and

$$\Delta_J = \frac{1}{\tau_2} \left(\frac{1}{\tau_1} + \frac{2\alpha' H^e}{c_1 N_d^e} \right) + 3\alpha'^2 c_2' \frac{(H^e)^4}{c_1 (N_d^e)^2}$$

Since $T_J < 0$ and $\Delta_J > 0$, the equilibrium point (H^e, N_d^e) is a stable node or a stable focus (spiral) according to the sign of $(T_J^2 - 4\Delta_J)$. We note that if the value of $\alpha' c_2'$ does not satisfy the above constraint, then T_J can be negative, which means that Eq. (1) describes an unstable dynamical system. In addition, since the sign of T_J never changes, there is no local bifurcation. A similar analysis that corroborates the above result has been performed recently by Jiang and Wang (2014).

2.4. Existence of limit cycles

One of the important points of this paper is the possibility of limit cycle solutions of the KF11 delay differential equations (DDEs). This needs rigorous examination. First, we note that the KF11 equations with constant delay T do not have any limit cycle solutions with period T. To see this, we consider either the Bendixson-Dulac theorem or the special case known as Bendixson's criterion (*e.g.* Minorsky, 1962; Glansdorff and Prigogine, 1971). To illustrate the use and consequences of this theorem to the problem at hand, we first rewrite the KF11 system: $\mathrm{d}H/\mathrm{d}t = f[H(t-T), N_d(t-T)]$ and $\mathrm{d}N_d/\mathrm{d}t = g[H(t-T), N_d(t-T)]$, where the functions f and g are

given by the rhs (right hand sides) in Eq. (1). The Bendixson-Dulac theorem may be applied to this system by considering the sign of the expression $\partial_H(\phi f) + \partial_{N_d}(\phi g)$, where $\phi(H, N_d) = 1$ (this case is Bendixson's criterion).

Now, suppose that this set of equations has a non-constant T-periodic solution $[H(t), N_d(t)]$. Then, it follows that $\mathrm{d}H/\mathrm{d}t = f[H(t), N_d(t)]$ and $\mathrm{d}N_d/\mathrm{d}t = g[H(t), N_d(t)]$. A simple calculation shows that $\partial_H(f) + \partial_{N_d}(g)$ is always negative. We can therefore conclude by the Bendixson-Dulac theorem that no solutions of period T exist in the simply connected region defined by positive values of H and N_d.

Since the KF11 equations are DDEs, a customary application of the Bendixson-Dulac theorem to prove the non-existence of limit cycles is inadequate. However, this theorem has been generalized (Busenberg and van den Driessche, 1993, Section 4) to higher dimensional ODEs, including DDEs like those proposed by KF11, for instance. This generalized "Bendixson-Dulac" theorem extends the concept of limit cycle to that of simple loop solutions, *i.e.* any continuous solution of the system of equations whose orbit contains a closed curve. Here, we apply this generalized theorem to the KF11 DDEs in order to demonstrate the absence of loop solutions.

To illustrate the use and consequences of this generalized theorem to the problem at hand, especially theorem 4.1 in Busenberg and van den Driessche (1993), we first rewrite the KF11 system:

$$\begin{cases} \dfrac{\mathrm{d}H}{\mathrm{d}t} &= F_1(H, N_d)\, h_t(H_t, N_{d,t}) + l_1(H, N_d) \\ \dfrac{\mathrm{d}N_d}{\mathrm{d}t} &= F_2(H, N_d)\, k_t(H_t, N_{d,t}) + l_2(H, N_d) \end{cases}$$

where $F_1(H, N_d) = -\alpha/c_1$, $F_2(H, N_d) = -\alpha c_2$, $h_t(H_t, N_{d,t}) = H_t^2/N_{d,t}$ and $k_t(H_t, N_{d,t}) = H_t^3$ are time-delayed functions (the subscript "t" stands for "time-delayed"), $l_1(H, N_d) = (H_0 - H)/\tau_1$, and $l_2(H_d, N_d) = (N_0 - N_d)/\tau_2$. Theorem 4.1 in Busenberg and van den Driessche (1993) gives conditions under which the KF11 DDEs have no simple loop solution. To verify the first condition, we define the vector function $g(H, N_d) = (g_1, g_2, 0)$. Here, $g_1 = \alpha\, c_2 A^3 + (N_0 - N_d)/\tau_2$, $g_2 = -\alpha\, A^2/(c_1 B) - (H_0 - H)/\tau_1$, A and B being constants. For notational simplicity, let (u, v) represent the coordinates of the

curve in Theorem 4.1 of Busenberg and van den Driessche (1993). Then:

$$\begin{aligned} g(H,N_d)\cdot\left(\frac{-\alpha u^2}{c_1 v}+l_1,-\alpha c_2 u^3+l_2,0\right) &= \frac{\alpha^2 c_2 A^2 u^2}{c_1}\left(\frac{u}{B}-\frac{A}{v}\right)+\alpha c_2 l_1\left(u^3+A^3\right) \\ &\quad -\frac{\alpha l_2}{c_1}\left(\frac{A^2}{B}+\frac{u^2}{v}\right) \\ &\leq 0 \end{aligned}$$

This follows from the following observations. The third term always contributes negatively, the second positively, to the sum. The first contributes negatively whenever $uv < AB$. Because c_1 is small, the first and third terms dominate the second so that, whenever $uv < AB$, the entire sum is negative. Since A and B can be taken as large as wished, the region is finally $\mathbb{R}^2_+$. To verify the second condition, we calculate $\partial_H g_2 - \partial_{N_d} g_1 = 1/\tau_1 + 1/\tau_2 > 0$ for any solution (H, N_d) in the region specified above. So, an application of the Busenberg-van den Driessche theorem implies that there is no simple loop solution traversed in the clockwise sense (the analogue for DDEs of the limit cycle of ODEs) for the positive values of H and N_d. A similar argument with vector function $-g$ works in the opposite sense as well. In other words, there is no solution of the KF11 system which enclose a smooth oriented simple closed curve.

3. A new species-competition bulk model

3.1. Description

In order to retain the simplicity of the KF11 model with ODEs instead of DDEs, we propose an approach which incorporates population competition, interaction, and carrying capacities in a natural way. Here, the populations are given by cloud water content $L_c\,(\mathrm{g\,cm^{-3}})$, rain water content $L_r\,(\mathrm{g\,cm^{-3}})$, and cloud droplet number concentration $N_d\,(\mathrm{cm^{-3}})$. We emphasize that these variables are considered here as macroscopic averages and that our model captures some of the macroscale properties of cloud-precipitation interactions by means of three relatively simple equations in three variables, rather than a fine-scale description with complete microphysical details. The model consists of three coupled differential equations, one each for L_c, L_r, and N_d. The system includes three main processes that contribute to the cloud budgets of

L_c, L_r, and N_d, namely: (1) sources/sinks which represent exchanges with the surroundings, and two internal processes, (2) autoconversion of cloud water to rain water, and (3) accretion of cloud water by rain water.

The various terms in the equations were suggested by the Seifert and Beheng (2001) parametrization for simulating autoconversion and accretion. Other terms can be added to the equations, such as self-collection for instance, but to retain some measure of simplicity we use only the terms already mentioned and which we describe further. This parametrization is a straightforward consequence of the stochastic collection equation (STE) with polynomial kernel. For this reason, it seems to us that this approach is more rigorous than many other methods which consist in using heuristic (or empirical) parametrizations. Details on the STE can be found in Seifert and Beheng (2001) and Pruppacher and Klett (1997) and references therein. It is worth mentioning that the goal of Seifert and Beheng (2001) has been to fill a gap between heuristic parametrizations and detailed microphysical (computationally expensive) schemes. The terms representing autoconversion and accretion are given by the following expressions (for a comprehensive overview see the references):

– Autoconversion: the contribution to dL_c/dt and dL_r/dt is given by

$$\left.\frac{dL_c}{dt}\right|_{auto} = -KL_c^4 N_d^{-2} = -\left.\frac{dL_r}{dt}\right|_{auto} \tag{4}$$

– Accretion: the contribution to dL_c/dt and dL_r/dt is given by

$$\left.\frac{dL_c}{dt}\right|_{accret} = -k_r L_c L_r = -\left.\frac{dL_r}{dt}\right|_{accret}. \tag{5}$$

We note that these expressions are adapted from the Seifert and Beheng (2001) parametrization by considering the variables as bulk, cloud-scale variables. The various parameters in the equations above are defined as follows: $K = [k_c/(20x^*)]\,(\nu+2)(\nu+4)(\nu+1)^{-2}$, where x^* is a cloud drop mass separating the cloud droplets from raindrops, k_c (k_r) is a constant from the cloud (rain) water kernel, and ν is the shape parameter of the gamma distribution. See Seifert and Beheng (2001) for complete details. By combining these equations, neglecting spatial dependence and adding source/sink terms for cloud and rain water contents, we arrive at the following system of bulk

coupled first-order differential equations for L_c, L_r and N_d:

$$\begin{cases} \dfrac{dL_c}{dt} &= A_c L_c - B_c(N_d) L_c^4 - k_r L_c L_r \\ \dfrac{dL_r}{dt} &= -A_r L_r + B_c(N_d) L_c^4 + k_r L_c L_r \\ \dfrac{dN_d}{dt} &= f(N_d, L_c, L_r) \end{cases} \tag{6}$$

Here, $B_c(N_d) = K N_d^{-2}$, and A_c and A_r are two positive constants that can be chosen so that the source/sink terms represent the background meteorological conditions. In particular, A_r represents the rain out process. These two constants give the timescales, $\tau_c = 1/A_c$ and $\tau_r = 1/|A_r|$, of cloud water content and rain water content evolutions respectively. In addition, $f(N_d, L_c, L_r)$ is a function which can be defined according to the question being investigated. Here, we choose to define f as follows:

$$\frac{dN_d}{dt} = A_c(N_0 - N_d) - \frac{4}{3} k_c L_c^2 - k_r L_r N_d. \tag{7}$$

On the rhs, the first term represents a supply of cloud droplets from the surroundings, N_0 being the background aerosol concentration that feeds the system (nucleation). Considered alone, this term causes an exponential increase (decrease) of N_d with N_0 as horizontal asymptote if initially N_d is lower (higher) than N_0. This represents cloud droplet concentration and when considered alone it tends toward a constant background aerosol population concentration. Moreover, this term (or similar ones) should be dominant in the very early stages of the cloud system evolution. Indeed, at the initial time (and close to $t = 0$), N_d is zero or very small (clear air condition) and must increase enough in order that the cloud can further evolve and produce rain. The two other terms in Eq. (7) come from Seifert and Beheng (2001, Eqs. A-5, A-6, and A-9) and represents respectively cloud droplet self-collection and accretion.

It has to be recalled that the state variables considered (L_c, L_r, and N_d) in this bulk model are macroscopic averages over the whole cloud. They can also be seen as local variables over a volume element of the cloud for which they are more or less uniform. A further step would be to introduce in the equation an explicit inside-cloud location (*e.g.* altitude z) dependence. Nonetheless, as showed below, the present model describes some macroscale features of could-precipitation coupling.

3.2. Comment on the form of the system of equations

We note that the first two equations in (6) constitute a predator-prey system modified to include autoconversion. To see this, observe that the constants $\{a, b, c, d\}$ in the Lotka-Volterra equations (Eq. 2) have the following formal correspondence with the model presented here: $\{a = A_c, b = -d = k_r, c = A_r\}$. Hence, the source/sink and accretion terms form a standard predator-prey system when considered alone. The quartic terms not only represent autoconversion of cloud droplets to rain given in the Seifert and Beheng (2001) parametrization, but also ensure that the cloud droplet population does not exhibit unbounded growth in the absence of competition. Thus, it plays a similar role to the carrying capacity term used in population dynamics to modify some of the unrealistic features of the original Lotka-Volterra system.

The entire system of equations is not rigorously equivalent to a three-species competition model. As already discussed, the first two equations constitute a modified Lotka-Volterra system. The autoconversion terms which modify the traditional predator-prey system have coefficients driven by the third equation, *viz.* that for N_d. The interpretation of the varying coefficients is that the carrying capacities of the water contents vary according to the state of N_d, which is more realistic for clouds.

It is worth mentioning that L_c and L_r are, for physical reasons, necessarily bounded. So, in virtue of the Poincaré-Bendixson theorem, the first two equations of system (6) have a solution that either converges towards a limit or presents an asymptotic behaviour that can take the form of a limit cycle. Boundedness has not been proved in a mathematical sense but, rather, we rely on numerical evidence (see some examples below, in Subsection 3.4) and on the fact that the present system of equations has much in common with other predator-prey models which are known to have bounded solutions. Obviously, if k_r and B_c are zero, the evolution of L_c is exponentially divergent. The terms involving non-zero values of k_r and B_c prevent unbounded evolution within certain parameter ranges, as is the case in predator-prey models. It is far beyond the scope of this paper to address rigorously (*i.e.* mathematically speaking) boundedness of solutions, but that could be formulated and explored deeply in a future specific work.

3.3. Stability analysis

3.3.1. Equilibrium points

The system

$$\left\{ \begin{array}{rcl} \dfrac{dL_c}{dt} & = & A_c L_c - B_c(N_d) L_c^4 - k_r L_c L_r \\ \dfrac{dL_r}{dt} & = & -A_r L_r + B_c(N_d) L_c^4 + k_r L_c L_r \end{array} \right. \tag{8}$$

has two equilibrium points $X_e = \{L_c^{(e)}, L_r^{(e)}\}$. In this section we treat N_d as a parameter. The first one is trivial: $X_e^{(1)} = 0$. There is no cloud nor *a fortiori* rain. Using Eq. (7), $N_d^{(e)} = N_0$, which means that the atmospheric volume considered has a constant CCN (cloud condensation nuclei) loading (that does not allow cloud formation). The second equilibrium point $X_e^{(2)}$ is such that:

$$A_c L_c^{(e)} = |A_r| L_r^{(e)} \quad \text{and} \quad B_c(N_d) \frac{|A_r|^3}{A_c^4} \left(L_r^{(e)}\right)^3 + \frac{k_r}{A_c} L_r^{(e)} - 1 = 0 \tag{9}$$

Since the two first terms of this third order polynomial are positive, there is only one real positive solution $L_r^{(e)}$ – the other two are complex conjugates. The expression of $N_d^{(e)}$ follows from those of $L_c^{(e)}$ and $L_r^{(e)}$ using Eq. (7) Plugging $L_c^{(e)}$ and $L_r^{(e)}$ into Eq. (7) yields:

$$N_d^{(e)} = \left(A_c + \frac{k_r A_c}{|A_r|} L_c^{(e)} \right)^{-1} \left[A_c N_0 - \frac{4}{3} k_c \left(L_c^{(e)}\right)^2 \right] \tag{10}$$

The eigenvalues of the jacobian matrix J of the system (6) are:

$$\lambda_\pm = \frac{1}{2} \left[T_J \pm \left(T_J^2 - 4\Delta_J \right)^{1/2} \right]$$

where the trace T_J and the determinant Δ_J of $[J]$ can be written as follows:

$$T_J = \mathrm{Tr}(J) = A_c - |A_r| + k_r \left(L_c^{(e)} - L_r^{(e)} \right) - 4 B_c(N_d) \left(L_c^{(e)}\right)^3 \tag{11}$$

and

$$\Delta_J = \det(J) = -A_c |A_r| + k_r \left(A_c L_c^{(e)} + |A_r| L_r^{(e)} \right) + 4 |A_r| B_c(N_d) \left(L_c^{(e)}\right)^3 \tag{12}$$

They must be evaluated for each of the two equilibrium points.

3.3.2. Stability analysis around $X_e^{(1)}$

In this case, $T_J = A_c - |A_r|$ and $\Delta_J = -A_c|A_r| < 0$. The two eigenvalues have opposite sign, $\lambda_+\lambda_- < 0$, with $\lambda_+ = A_c > 0$ and $\lambda_- = -|A_r| < 0$. The state $X_e^{(1)}$ is thus a saddle point.

3.3.3. Stability analysis around $X_e^{(2)}$

In this case

$$T_J = (3A_c + |A_r|)\left(\frac{k_r L_r^{(e)}}{A_c} - 1\right) \quad \text{and} \quad \Delta_J = -2A_c|A_r|\left(\frac{k_r L_r^{(e)}}{A_c} - \frac{3}{2}\right)$$

It follows that the equilibrium point $X_e^{(2)} = \left(L_c^{(e)}, L_r^{(e)}\right)$ is stable if:

$$\frac{k_r L_r^{(e)}}{A_c} < 1 \quad \text{i.e.} \quad L_r^{(e)} < \frac{A_c}{k_r} \quad \text{and} \quad L_c^{(e)} < \frac{|A_r|}{k_r} \tag{13}$$

Otherwise, for $k_r L_r^{(e)}/A_c > 1$, $X_e^{(2)}$ is an unstable equilibrium point.

The identity $k_r L_r^{(e)}/A_c = 1$, which separates a stable regime from an unstable one, has the straightforward consequence that $B_c \left[N_d^{(e)}\right] \left(L_c^{(e)}\right)^4 = 0$, *i.e.* $B_c = 0$ since $L_c^{(e)} \neq 0$. Physically, this critical value means that the net rate of the autoconversion process is zero: formation of a raindrop from cloud droplets only is compensated over a given time interval by the formation of cloud droplets from a raindrop only. Thus, the system maintains constant rain and cloud water contents whose values — see Eq. (13) — depend only on the exchange rates with the surroundings (A_c and A_r) and on the cloud-to-rain reaction constant (k_r). Below the critical value ($B_c < 0$), the autoconversion process results in net production of cloud droplets from raindrops. It constitutes a nonlinear amplification term for cloud droplets and a nonlinear damping term for raindrops, *i.e.* disturbances from equilibrium grow. In other words, the cloud is growing such that cloud droplets become more numerous while the number of raindrops vanishes. This behavior is reversed above the critical value ($B_c > 0$): the non linear term compensates any deviation from the equilibrium point (stability). In the case $B_c < 0$, without any cloud-rain interaction ($k_r = 0$), cloud (rain) water content is an increasing (decreasing) function.

The other characteristic value is $k_r L_r^{(e)}/A_c = 1.5$. Below (above) this value, Δ_J is positive (negative). So $X_e^{(2)}$ is a saddle point if $L_r^{(e)} = 1.5A_c/k_r$.

The nature (node, focus or spiral) of $X_e^{(2)}$ is provided by the sign of $T_J^2 - 4\Delta_J$:

$$T_J^2 - 4\Delta_J = \left[(3A_c + |A_r|)^2 \left(\frac{k_r L_r^{(e)}}{A_c} - 1 \right)^2 \right] + 4|A_r|A_c \left(2\frac{k_r L_r^{(e)}}{A_c} - 3 \right)$$

If $k_r L_r^{(e)}/A_c = 1$, $T_J^2 - 4\Delta_J = -4|A_r|A_c < 0$ which means that $X_e^{(2)}$ is a focus.

For $k_r L_r^{(e)}/A_c \neq 1$, the sign of $T_J^2 - 4\Delta_J$ depends on the number $\mathcal{N}_\tau = |A_r|/A_c$ through the second order polynomial equation:

$$(3A_c + |A_r|)^2 \left(\frac{k_r L_r^{(e)}}{A_c} \right)^2 - 2 \left(\frac{k_r L_r^{(e)}}{A_c} \right) \left[(3A_c + |A_r|)^2 - 4A_c|A_r| \right] + (|A_r| - 3A_c)^2$$

The two solutions are easy to find:

$$Z_\pm = \frac{(3A_c + |A_r|)^2 - 4|A_r|A_c}{(3A_c + |A_r|)^2} \pm \frac{2\left[(9A_c^2 + |A_r|A_c)\left(|A_r|^2 + A_c|A_r| \right) \right]^{1/2}}{(3A_c + |A_r|)^2}$$

Three cases can be distinguished at first sight:

- $|A_r| = A_c$: so $Z_\pm = (3 \pm \sqrt{5})/4 > 0$. Between these two values, $T_J^2 - 4\Delta_J < 0$, so that $X_e^{(2)}$ is a focus. Outside of this interval, we have a node
- $|A_r| \gg A_c$: so $Z_\pm = 1 \pm 2\left(A_c/|A_r| \right)^{1/2} > 0$. Same as previously.
- $|A_r| \ll A_c$: so $Z_\pm = 1 \pm (2/3)\left(|A_r|/A_c \right)^{1/2} > 0$. Same as previously.

3.3.4. Andronov-Hopf bifurcation

It follows from what precedes that the eigeinvalues of the jacobian matrix cross the imaginary axis for $B_c = 0$. At this point, they are pure imaginary numbers, $\lambda_\pm = i(A_c|A_r|)^{1/2}$. There, the system has a limit cycle. Just after ($B_c < 0$), the spiral is unstable whilst it is stable just before ($B_c > 0$). This behavior is precisely a *Hopf bifurcation*: an unstable focus gives birth to a stable focus (and *vice versa*) through a limit cycle. The existence of such a bifurcation is an important point for further investigations of cloud organization in a coupled-cloud field at the mesoscale (Kuramoto, 2003).

3.4. Examples

We now illustrate the behavior of this set of three equations with some examples. The values chosen for k_r and k_c are those given in Seifert and Beheng (2001) which follow from approximations to the collection kernel in Long

(1974), *i.e.* $k_c \approx 5.66 \times 10^{11}\,\mathrm{cm^3\,g^{-2}\,min^{-1}}$ and $k_r \approx 3.47 \times 10^{5}\,\mathrm{cm^3\,g^{-1}\,min^{-1}}$. The value of $x^* = 2.6 \times 10^{-7}\,\mathrm{g}$, following Seifert and Beheng (2001). We take $\nu = 2$, which is a typical value for warm clouds (*e.g.* , Pruppacher and Klett, 1997, chap. 2). With these values, the parameter $K \approx 2.905 \times 10^{17}\,\mathrm{cm^3\,g^{-3}\,min^{-1}}$.

In addition, we take $A_c = 0.02\,\mathrm{min^{-1}}$ and $A_r = 0.1\,\mathrm{min^{-1}}$. So, cloud water content and rain water content are expected to evolve on the timescales $\tau_c = 50\,\mathrm{min}$ and $\tau_r = 10\,\mathrm{min}$. The latter is lower than the former since raining out is a rapid process compared to the evolution of cloud water content. These values are chosen for illustrative purposes.

3.4.1. First example: periodic behavior

We choose as initial conditions $N_d(0) = 10\,\mathrm{cm^{-3}}$, $L_c(0) = 10^{-9}\,\mathrm{g\,cm^{-3}}$, $L_r(0) = 0$, and $N_0 = 50\,\mathrm{cm^{-3}}$. The system exhibits oscillatory behavior after approximately 300 min, with a period of about 200 min, which is physically realistic (Fig. 2a). Both N_d and L_c increase initially (the former faster than the latter) until rain appears. Soon thereafter, rain water content peaks and droplet number and mass concentration decrease drastically in a short interval of time. Minimum values of L_c are reached and rain water content decreases to zero. Then N_d and L_c start to increase again, and so on. This periodicity appears clearly as a limit cycle on the plot (L_c, L_r) displayed in Fig. 2b. It is interesting to mention that peaks in rain water content are delayed from L_c peaks by about $20 - 30\,\mathrm{min}$, which is a very realistic value for rain to form from a cloud droplet by collection (Fig. 2c). We also note that similar oscillations and limit cycles are obtained for other initial conditions (not shown). Note that the model presented here represents well a timescale of precipitation production that has to be explicity and arbitrarily accounted for *via* delays in the more complicated DDE framework.

3.4.2. Second example: damped behavior

If N_0 is lower than $N_d(0)$, the feeding of the system is not sufficient to maintain the cloud-rain system in a harmonic (or quasi) oscillation and a damping is observed (Fig. 3): N_d, L_c, and L_r still oscillate but their respective amplitudes decrease progressively until a steady state is reached. Initially N_d decreases exponentially as expected, and then decreases more rapidly when L_c and L_r peak for the first time.

Damping can also be obtained by introducing in the model a decreasing evolution for the CCN supply, for instance $N_0 = 50\exp(-0.002\,t)$. This

means that the initial CCN burden is divided by around 2.72 in 500 min, *i.e.* 8 hours. Keeping the same initial conditions as previously, we get the behavior displayed in Figure 4, which is typical of a damped oscillator: N_d increases until a certain time t (approximately 120 min) at which the exponential function becomes significant. Then N_d decreases dramatically. The same behavior is seen for L_c and L_r which increase until $t = 500$ min and then exhibit decaying amplitude oscillations that eventually ($t > 1\,500$ min) die out. Again, we note that the peaks of L_r are delayed with respect to those of L_c by about $20 - 30$ min.

The same damping behavior is observed (not shown) for different initial conditions, in particular if $L_r \neq 0$, provided the values are realistic.

4. Discussion and conclusion

Certain aspects of a system's bulk behavior arise out of many small-scale interactions. These aspects may be investigated with simple models that faithfully represent the bulk behavior, but do not consider directly the full complexity of the system. In conjunction with more detailed models and simulations, models which represent bulk behavior can also enhance our understanding of complex dynamical systems. The model presented here, which has aspects of species competition in biology, is a tool with which to examine the complexity of cloud-rain interactions in a way that highlights certain aspects of their behavior in a simple but realistic manner. This model is not meant to supplant more detailed simulations of cloud-precipitation interactions but to represent certain predictable elements of the macrobehavior of the full complex dynamical system.

In the first part of the paper, we examined some important mathematical properties of the KF11 DDEs model which is a similar model devoted to analyze the bulk behavior of a cloud-rain system. The focus has been put on scaling and limit cycles or loop solutions. In particular, it has been shown, through the Busenberg theorem that this model has no proper limit cycle solutions. The model we have introduced in this paper (second part) is another point of view which retains the idea of modeling cloud-precipitation interaction through population dynamics and exhibits predator-prey behavior with rain as predator and cloud droplets as prey. The stability analysis has shown that our model has limit cycles and a Hopf bifurcation.

In particular, the model formulated here is a system of ODEs rather than DDEs. It is derived from a physically-based parametrization. Several

examples illustrate that our model reproduces realistically the behaviour of an unique cloud-rain system. In particular, rain water content peaks are delayed by about $20 - 30\,\mathrm{min}$ with respect to cloud water content peaks. Some of the novel properties of the model include regions of parameter space in which clouds grow at the expense of rain and *vice versa* as determined from bifurcation analysis.

Further properties of our model such as ability to represent various physical situations, and sensitivity tests to parametrization schemes similar to those performed by Wacker (1995) for mixed and ice clouds, will be explored in more detail in future work. Due to its properties, this cloud-rain model is intended to be further developed for examination of cloud organization at larger scales in a coupled-cloud field.

Acknowledgements

We are very grateful to the Fulbright Committee which, by means of funding for United States-France scientific researcher exchanges, facilitates our collaboration and permits our investigations in Statistical Physics for Atmospheric Cloud Systems (SPACS group).

Appendix 1: Unit analysis

The system (1) is derived from four empirical equations which we have summarized in Table 1 together with their numbering in KF11.

Eq. number in KF11	Equation	Constants
[2]	$LWP = 0.5\, c_1 H^2$	$c_1 = 2 \times 10^{-6}\,\mathrm{mm\,m^{-2}}$
[5]	$\mathrm{d}LWP/\mathrm{d}t = -R$	None
[4]	$R = \alpha H^3 N_d^{-1}$	$\alpha = 2\,\mathrm{mm\,m^{-6}\,d^{-1}}$
[9]	$\mathrm{d}N_d/\mathrm{d}t = -c_2 N_d R$	$c_2 = 0.3\,\mathrm{m^{-1}}$

TAB. 1 – *Equations and constants in KF11 discussed here. In KF11, LWP and R are liquid water path and rainrate, respectively. The corresponding units are explicitely* $\mathrm{g\,m^{-2}}$ *and* $\mathrm{mm\,d^{-1}}$.

Eq. [2] connects liquid water path (LWP, in $\mathrm{g\,m^{-2}}$) with cloud depth (H, in m). The dimension of LWP is $[M][L]^{-2}$ (where $[M]$ and $[L]$ are mass and length dimensions), which implies that the dimension of c_1 is $[M][L]^{-4}$

and not $[L]^{-1}$ (cf. Table 1). Indeed, the well-established relationship is given by $LWP\,(\mathrm{g\,m^{-2}}) = 0.5\,c_w H^2$, where $c_w = 2 \times 10^{-6}\,\mathrm{kg\,m^{-4}}$ (*e.g.* Geoffroy et al., 2008). Actually, $c_w = \rho_w c_1$, where $\rho_w \approx 10^3\,\mathrm{kg\,m^{-3}}$ is liquid water density and $c_1 = 2 \times 10^{-9}\,\mathrm{m^{-1}}$ — in Tab. 1, $c_1 = 2 \times 10^{-6}\,\mathrm{mm\,m^{-2}}$, *i.e.* $c_1\,(\mathrm{m^{-1}}) = 10^{-3}\,c_1\,(\mathrm{mm\,m^{-2}})$. The relationship between LWP and H we get is thus:

$$\begin{aligned} LWP\,(\mathrm{g\,m^{-2}}) &= \frac{1}{2} c_w\,(\mathrm{kg\,m^{-4}})\,H^2\,(\mathrm{m^2}) \\ &= \frac{1}{2}\,\rho_w\,(\mathrm{kg\,m^{-3}})\,c_1\,(\mathrm{m^{-1}})\,H^2\,(\mathrm{m^2}) \end{aligned} \tag{14}$$

If we look now at Eq [5] and the units chosen, the decreasing rate of LWP due to rain cannot equal exactly the rainrate R (in $\mathrm{mm\,d^{-1}}$). In fact, $\mathrm{d}LWP/\mathrm{d}t$ is proportional to the precipitation flux density (or rain current $J_r = -\rho_w R$). The coefficient of proportionality is determined by the choice of units. If, as in KF11, we express time in minutes (it is the most natural timescale for cloud macroscopic physics), and keep LWP in $\mathrm{g\,m^{-2}}$ as above, we obtain:

$$\begin{aligned} \frac{\mathrm{d}LWP}{\mathrm{d}t}\,(\mathrm{g\,m^{-2}\,min^{-1}}) &= -\rho_w\,(\mathrm{g\,m^{-3}})\,R\,(\mathrm{m\,min^{-1}}) \\ &= -10^3\,\rho_w\,(\mathrm{kg\,m^{-3}})\,R\,(\mathrm{m\,min^{-1}}) \\ &= -\frac{10^3}{60 \times 24}\,\rho_w\,(\mathrm{kg\,m^{-3}})\,R\,(\mathrm{m\,d^{-1}}) \\ &= -\frac{1}{60 \times 24}\,\rho_w\,(\mathrm{kg\,m^{-3}})\,R\,(\mathrm{mm\,d^{-1}}) \end{aligned} \tag{15}$$

since $R\,(\mathrm{m\,min^{-1}}) = 10^{-3}\,R\,(\mathrm{mm\,d^{-1}})/(60 \times 24)$. Combining Eqs. (14) and (15) yields:

$$\begin{aligned} \frac{\mathrm{d}H}{\mathrm{d}t}\,(\mathrm{m\,min^{-1}}) &= \frac{\mathrm{d}LWP/\mathrm{d}t\,(\mathrm{g\,m^{-2}\,min^{-1}})}{c_w\,(\mathrm{kg\,m^{-4}})\,H\,(\mathrm{m})} \\ &= -\frac{\rho_w\,(\mathrm{kg\,m^{-3}})\,R\,(\mathrm{mm\,d^{-1}})}{(60 \times 24)\,c_w\,(\mathrm{kg\,m^{-4}})\,H\,(\mathrm{m})} \\ &= -\frac{1}{60 \times 24}\,\frac{R\,(\mathrm{mm\,d^{-1}})}{c_1\,(\mathrm{m^{-1}})\,H\,(\mathrm{m})} \\ &= -\frac{10^3}{60 \times 24}\,\frac{R\,(\mathrm{mm\,d^{-1}})}{c_1\,(\mathrm{mm\,m^{-2}})\,H\,(\mathrm{m})} \end{aligned} \tag{16}$$

370 It is possible, although not common, to divide LWP by ρ_w and then to de-
371 fine a volumetric liquid water path: $LWP_v\,(\mathrm{m}) = 10^{-3}\,LWP\,(\mathrm{g\,m^{-2}})/\rho_w\,(\mathrm{kg\,m^{-3}})$.

In this case, Eqs. [2] and [5] of Table 1 are correct provided that, for Eq. [5], R be expressed in $\mathrm{m\,min^{-1}}$, or equivalently, considering $10^{-3}\,R\,(\mathrm{mm\,d^{-1}})/(60\times 24)$. However, we have not found any explicit mention of LWP in m or mm in KF11 and further papers; there LWP is explicitly expressed in $\mathrm{g\,m^{-2}}$ several times.

The KF11 model also employs two parametrizations which relate R, N_d, and $\mathrm{d}N_d/\mathrm{d}t$ (see Eqs. [4] and [9] in Table 1). The units of the latter two quantities are naturally $\mathrm{cm^{-3}}$ and $\mathrm{cm^{-3}\,min^{-1}}$, respectively. According to the units used in KF11, the rhs of Eq. [4] is in $\mathrm{mm\,m^{-3}\,cm^{3}\,d^{-1}}$, while the lhs (left hand side) is in $\mathrm{mm\,d^{-1}}$. Although Eq. [4] is dimensionally correct ($[L][T]^{-1}$, where $[T]$ is the time dimension), the units of the rhs and lhs are not the same. Indeed, the relation $R=\alpha H^3/N_d$ should have N_d in $\mathrm{m^{-3}}$ when H is in m. If we choose to express N_d in $\mathrm{cm^{-3}}$, then we must multiply H^3/N_d by 10^{-6}. With the unit of α, R is thus in $\mathrm{mm\,d^{-1}}$:

$$R\,(\mathrm{mm\,d^{-1}}) = 10^{-6}\,\alpha\,(\mathrm{mm\,m^{-6}\,d^{-1}})\,H^3\,(\mathrm{m^3})\,N_d^{-1}\,(\mathrm{cm^3}) \tag{17}$$

Thus, for Eq. (16), we obtain:

$$\frac{\mathrm{d}H}{\mathrm{d}t}\,(\mathrm{m\,min^{-1}}) = -\frac{10^{-3}}{60\times 24}\,\frac{\alpha\,(\mathrm{mm\,m^{-6}\,d^{-1}})\,H^2\,(\mathrm{m^2})}{c_1\,(\mathrm{mm\,m^{-2}})\,N_d\,(\mathrm{cm^{-3}})} \tag{18}$$

In addition, Wood (2006) (ref. 20 in KF11) gives a value of c_2 which does not correspond to that used in KF11. Aside from the conflation of rain current and rainrate in Wood (2006) — this article seems to use P as rainrate and divides it by liquid water density (ρ_w), whereas P should be the rain current and P/ρ_w the rainrate —, the coefficient of proportionality between $\mathrm{d}N_d/\mathrm{d}t$ and R is $3E_0/4 = 3\times 10^3\,\mathrm{m^{-1}}$ since $E_0 = 4\times 10^3\,\mathrm{m^{-1}}$. This value is different from the $0.3\,\mathrm{m^{-1}}$ used in KF11 (assuming that P, in Wood (2006), is rainrate, and not rain current, which is very few probable due to a dimensional analysis of the Eq. 14 of Wood (2006), c_2 would be $3\,\mathrm{m^{-1}}$, *i.e.* the previous value of c_2 divided by ρ_w, which is again different from the value of Table 1). Because, in Eq. [9], $\mathrm{d}N_d/\mathrm{d}t$ has to be in $\mathrm{cm^{-3}\,min^{-1}}$, we have:

$$\frac{\mathrm{d}N_d\,(\mathrm{cm^{-3}\,min^{-1}})}{\mathrm{d}t} = c_2\,N_d\,(\mathrm{cm^{-3}})\,R\,(\mathrm{m\,min^{-1}}) \tag{19}$$

with $c_2 = 3\times 10^3\,\mathrm{m^{-1}}$.

Then, because $R\,(\mathrm{m\,min^{-1}}) = 10^{-3}\,R\,(\mathrm{mm\,d^{-1}})/(60\times 24)$, we obtain, by substituting the rainrate of Eq. (17) into Eq. (19):

$$\frac{\mathrm{d}N_d\,(\mathrm{cm^{-3}\,min^{-1}})}{\mathrm{d}t} = \frac{10^{-9}}{60\times 24}\,c_2\,(\mathrm{m^{-1}})\,\alpha\,(\mathrm{mm\,m^{-6}\,d^{-1}})\,H^3\,(\mathrm{m^3}) \tag{20}$$

Finally, with this set of units, *i.e.* with H and N_d in m and cm^{-3} respectively, and time in minutes, the consistent (in terms of units) system of equations we get is:

$$\begin{cases} \dfrac{\mathrm{d}H}{\mathrm{d}t} &= \dfrac{H_0 - H}{\tau_1} - \dfrac{10^{-3}}{60 \times 24} \dfrac{\alpha H^2 (t-T)}{c_1 N_d (t-T)} \\ \dfrac{\mathrm{d}N_d}{\mathrm{d}t} &= \dfrac{N_0 - N_d}{\tau_2} - \dfrac{10^{-9}}{60 \times 24} \alpha c_2 H^3 (t-T) \end{cases} \tag{21}$$

with $c_1 = 2 \times 10^{-6}\,\mathrm{mm\,m^{-2}}$, $c_2 = 3 \times 10^3\,\mathrm{m^{-1}}$, $\alpha = 2\,\mathrm{mm\,m^{-6}\,d^{-1}}$. If we consider that LWP is a volumetric liquid water path, as it might be assumed as suggested above, and R in $\mathrm{mm\,d^{-1}}$, the factor 10^{-3} is replaced by 10^3.

Appendix 2: Other empirical parametrizations

Other empirical parametrizations can also be used to relate H, N_d, and R. Here, we would like to suggest three. In particular, we can introduce the following three alternative parametrizations for the delay term $\mathrm{d}N_d/\mathrm{d}t$ instead of the one in Wood (2006). (*i*) The empirical relationship proposed in Mechem et al. (2006, Eq. 9): $\mathrm{d}N_d/\mathrm{d}t\,(\mathrm{cm^{-3}\,d^{-1}}) = -69.4\,(N_d R)^{0.668}$, with N_d in $\mathrm{cm^{-3}}$ and R in $\mathrm{cm\,d^{-1}}$. (*ii*) The following empirical relationships given in Geoffroy et al. (2008): $J_r\,(10^{-6}\,\mathrm{kg\,m^{-2}\,s^{-1}}) = a\,(LWP^{\alpha}/N_d) - b$. Here, LWP is in $\mathrm{g\,m^{-2}}$, a, b, and α are positive constants that take the values summarized in Table 2.

a	α	b
0.3×10^6	2	10^{-6}
24.37×10^9	1	0
21.5×10^3	1.5	2.3×10^{-6}

TAB. 2 – *Values of the constants in Geoffroy et al. (2008)*

When using this parametrization, it is necessary to first use Eq. (14) to change LWP into H.

(*iii*) Finally, a parametrization of the delay term $\mathrm{d}N_d/\mathrm{d}t$ by taking

$$\frac{N_d}{LWP}\frac{\mathrm{d}LWP}{\mathrm{d}t} = \frac{2N_d}{H_r}\frac{\mathrm{d}H_r}{\mathrm{d}t} \tag{22}$$

This follows from Eq. (14). The equation for $\mathrm{d}H_r/\mathrm{d}t$ can then be substituted into this equation to complete the parametrization. This equation with delay

is finally substituted for the delay term in the second equation in the KF11 system.

When using these different parametrizations, a set of coupled first-order DDEs similar to Eq. (1) is obtained. The units must be made consistent when the various empirical relationships are employed. Namely, H is in m, N_d is in cm^{-3}, and time is expressed in minutes. For the numerical tets we have performed, these parametrizations have given results similar to those in Figure 1. However, we have not made a complete test of sensitivity of the model to changes in parametrization since it is not the purpose of this paper. Our goal here is to suggest other possibilities to parametrize cloud-rain interaction processes that could be investigated more deeply in future research.

Busenberg, S., van den Driessche, P., 1993. A method for proving the non-existence of limit cycles. Jour. Math. Anal. Appl. 172, 463–479.

Engelborghs, K., Luzyanina, T., Roose, D., 2000. Numerical bifurcation analysis of delay differential equations. Jour. Comp. Appl. Math. 125, 265–275.

Feingold, G., Koren, I., 2013. A model of cloupled oscillators applied to the aerosol-cloud-precipitation system. Nonlin. Processes Geophys. 20, 1011–1021.

Feingold, G., Koren, I., Wang, H., Xue, H., A., B., 2010. Precipitation-generated oscillations in open cellular cloud fields. Nature Letters 466, 849–852.

Geoffroy, O., Brenguier, J.-L., Sandu, I., 2008. Relationship between drizzle rate, liquid water path and droplet concentration at the scale of a stratocumulus cloud system. Atmos. Chem. Phys. 8, 4641–4654.

Glansdorff, P., Prigogine, I., 1971. Structure, stabilité et fluctuations. Masson et Cie.

Held, I., 2005. The gap between simulation and understanding in climate modeling. Bull. Am. Meteor. Soc., 1609–1614.

IPCC, ., 2013. Climate Change 2013: The Physical Science Basis. Contribution of Working Group I to the Fifth Assessment Report of the Intergovernmental Panel on Climate Change.

Jiang, Q., Wang, S., 2014. Aerosol Replenishment and Cloud Morphology: A VOCALS Example. Journal of the Atmospheric Sciences 71, 300–311.

Koren, I., Feingold, G., 2011. Aerosol-cloud-precipitation system as a predator-prey problem. PNAS 108, 12227–12232.

Koren, I., Tziperman, E., Feingold, G., 2017. Exploring the nonlinear cloud and rain equation. Chaos 27, 013107–1–013107–9.

Kuramoto, Y., 2003. Chemical Oscillations, Waves, and Turbulence. Dover Publications.

Lipowski, A., Lipowska, D., 2000. Nonequilibrium phase transition in a lattice prey-predator system. Physica A 276, 456–464.

Long, A. B., 1974. Solutions to the Droplet Collection Equation for Polynomial Kernels. J. Atm. Sci. 31, 1040–1052.

Mechem, D. B., Robinson, P. C., Kogan, Y. L., 2006. Processing of cloud condensation nuclei by collision-coalescence in a mesoscale model. Journal of Geophysical Research: Atmospheres 111, d18204.

Minorsky, N., 1962. Nonlinear Oscillations. Van Nostrand.

443 Mülmenstädt, J., Feingold, G., 2018. The Radiative Forcing of Aerosol–Cloud
444 Interactions in Liquid Clouds: Wrestling and Embracing Uncertainty. Cur-
445 rent Climate Change Reports 4, 23–40.
446 Pruppacher, H., Klett, J., 1997. Microphysics of Clouds and Precipitation.
447 Atmospheric and Oceanographic Sciences Library. Springer Netherlands.
448 Seifert, A., Beheng, K. D., 2001. A double-moment parameterization for si-
449 mulating autoconversion, accretion and selfcollection. Atmos. Res. 59-60,
450 265–281.
451 Wacker, U., 1995. Competition of precipitation particles in a model with
452 parametrized cloud microphysics. J. Atmos. Sci. 52, 2577–2589.
453 Wood, R., 2006. Rate of loss of cloud droplets by coalescence in warm clouds.
454 J. Geophys. Res. 111, 1–6.

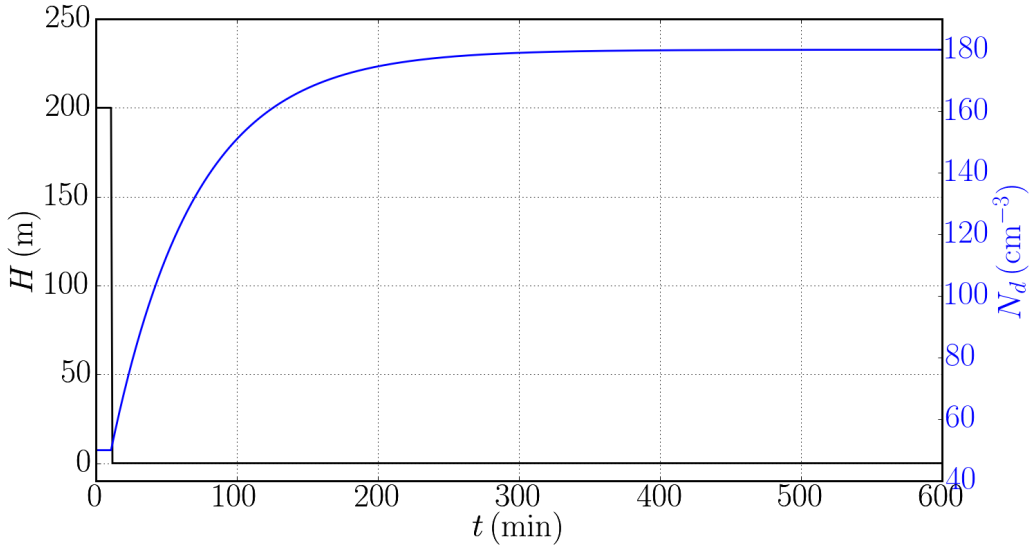

FIG. 1 – *Evolution of H and N_d according to system (1) with $H_0 = 530\,\mathrm{m}$, $N_0 = 180\,\mathrm{cm}^{-3}$, $\tau_1 = \tau_2 = 60\,\mathrm{min}$, and $T = 12\,\mathrm{min}$. Initial conditions are $H(t = 0) = 200\,\mathrm{m}$ and $N_d(t = 0) = 50\,\mathrm{cm}^{-3}$. We have used the pydelay package of Python.*

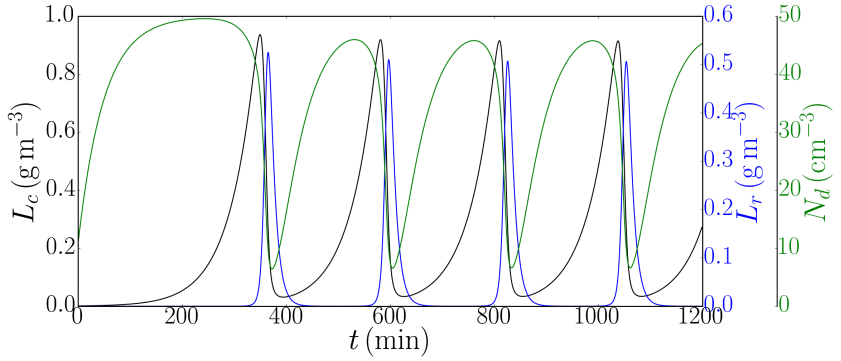

a

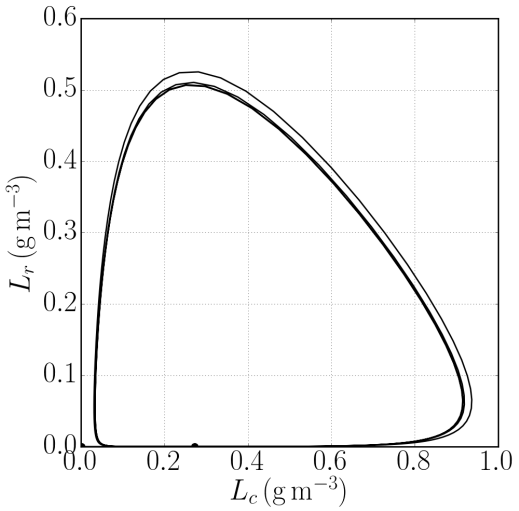

b

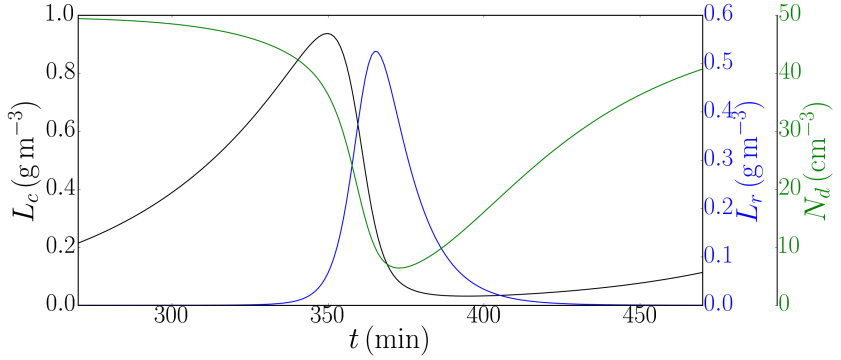

c

FIG. 2 – *Evolution of N_d, L_c and L_r (a) and limit-cycle in the configuration space (L_c, L_r) (b) for the initial conditions and values of parameters given in the text. On the limit cycle, initial and final time of integration are at the origin and $(0.25, 0)$ respectively. (c) Zoom of (a).*

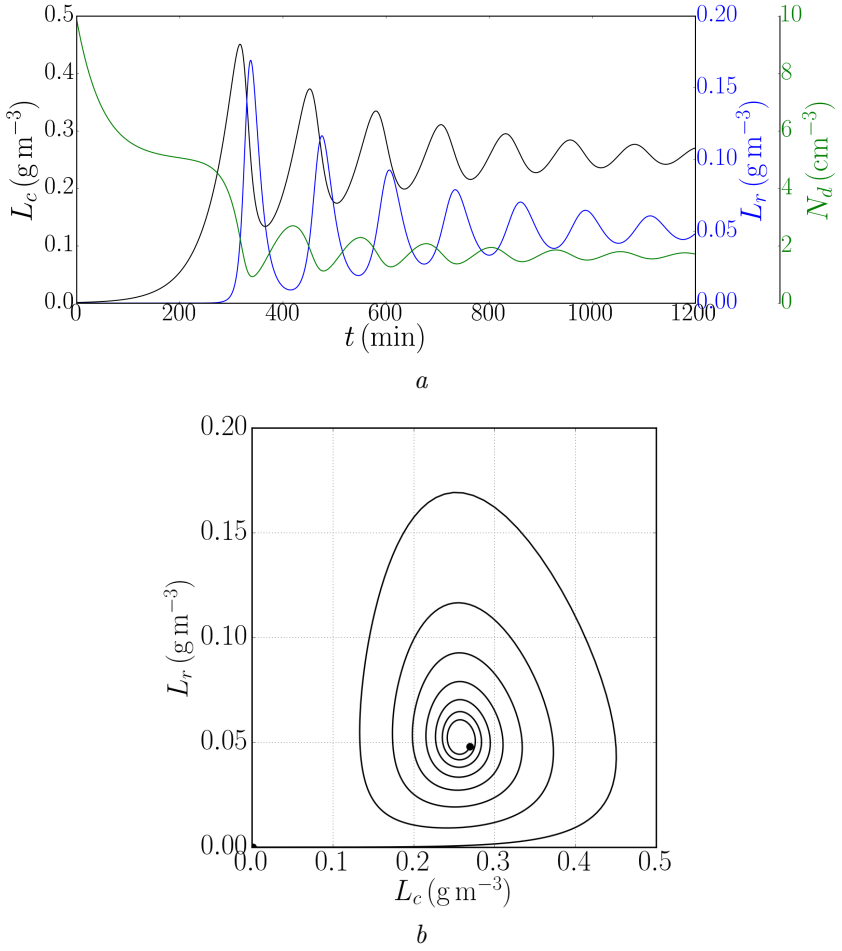

FIG. 3 – *Same as Fig. 2 but for* $N_0 = 5\,\mathrm{cm}^{-3}$. *On the limit cycle, initial time of integration is at the origin and final time of integration is represented by the black small ball at about* $(0.28, 0.05)$.

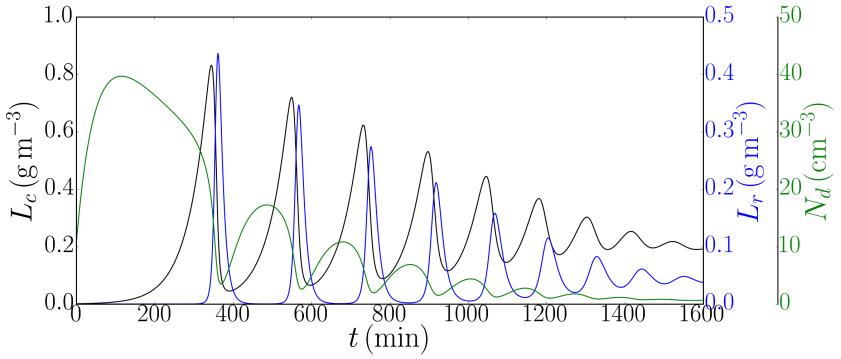

a

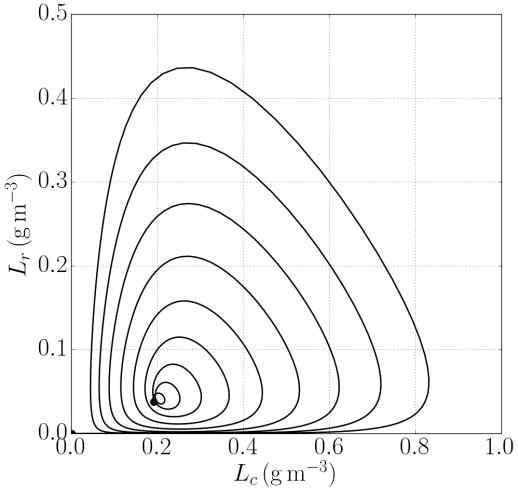

b

FIG. 4 – *Another kind of damped cloud system. On the limit cycle, initial time of integration is at the origin and final time of integration is represented by the black small ball at about* $(0.2, 0.05)$.